Proceedings of the ASME 2010 3rd Joint US-European Fluids Engineering Summer Meeting and 8th International Conference on Nanochannels, Microchannels, and Minichannels
FEDSM-ICNMM2010
August 1-5, 2010, Montreal, Canada

FEDSM-ICNMM2010-30452

Study On Performance of Canned Motor Pump Based on Numerical Simulation

Shuiqing Zhou
Fluid Machinery Research Center,
Jiangsu University, China

Fanyu Kong
Fluid Machinery Research Center,
Jiangsu University, China

Ting Wang
Fluid Machinery Research Center,
Jiangsu University, China

Wenting Wang
Fluid Machinery Research Center,
Jiangsu University, China

ABSTRACT

The pressure fluctuations in a centrifugal pump at both design and off-design points and the internal electromagnetic field of canned motor are presented in this paper. The 3D unsteady flow numerical simulation is completed at different operating points by using the FLUENT. A sliding mesh technique is applied to take into account the impeller-volute interaction. The FFT technology is adopted to process those dynamic pressure data to reveal the frequency features. All the power spectrum results present that the pressure fluctuation amplitude of blade suction side is greater than the one of blade pressure side. Some unknown high-frequency contents are discovered in the flow field. Meanwhile, the canned motor designed are applied by the design method of permanent magnet synchronous motor. The internal electromagnetic field of the motor is simulated with the ANSOFT software. Magnetic field analysis is carried out between two different magnetic circuit structure: U-type and inverted U-type. Comparing to U-type magnetic circuit structure, the latter is more conducive to reduce the magnetic flux leakage in the iron core tooth.

Keywords: Canned Motor , Centrifugal Pump, Electromagnetic Field, Pressure Fluctuation

INTRODUCTION

Canned motor pump is a kind of zero leakage pumps which gathered the canned motor and the centrifugal pump in one union. Canned motor pump is mainly applied in important fields such as military industry and space industry, and used to pump fluid which is poisonous, corrosive, volatile, precious or easy to vaporize, volatilize and explode(Kong et al,2003,2006). However, the efficiency of general canned motor is lower. With the application of permanent magnet synchronous technology, the performance of canned motor could be improved. In reality, it is difficult to determine the internal magnetic circuit structure of canned motor during the design process. In particular, it is not easy to carry out performance test among different types of permanent magnet rotor . The price of permanent magnetic materials ,as it has come to be known, was relatively expensive .

Simultaneously, this class of pumps generates a dynamic pressure component along with the static pressure component. The dynamic pressure component, called pressure fluctuation and rides on top of the static pressure component like an AC signal, is composed of the effects of suction and discharge recirculation, blade inlet rotating stall, rotor-stator interaction, cavitation , and excessive wear ring leakage, etc. Therefore, the pressure fluctuations at various running conditions conceal many flow contents including but not limited to those mentioned above(Chen et al,2007). It is further believed that analyzing the pressure fluctuations is able to realize the monitoring of those dynamic effects such as the flow patterns and flow structures in the coming future.

With the development of CFD and computer technology, the method of numerical simulation has widely been used for pump design. In this work the electromagnetic fields of two different magnetic circuit structure in permanent magnet canned motor are numerically displayed. At the same time, the pressure fluctuations in the centrifugal pump are obtained by 3D unsteady flow numerical simulations.

NOMENCLATURE

B_r	Residual magnetic flux density of magnets, *T*
b_2	Outlet width of impeller, *mm*
b_3	Volute inlet width, *mm*
C_p	Pressure coefficient
D_1	Impeller inlet diameter, *mm*
D_2	Impeller outside diameter, *mm*
H	Head, *m*
n	Motor synchronous speed, *r/min*
P	Motor rated power , *kW*

p Static pressure, *pa*
Q Design point flowrate, m^3/h
Q_d Off-design point flowrate , m^3/h
U_2 Impeller outlet circumferential speed, *m/s*
δ Air gap length of motor, *mm*
Z Blade number of impeller
ρ Density, kg/m^3

STRUCTURE OF PERMANENT MAGNET CANNED MOTOR PUMP

Figure 1 shows the structure of permanent magnet canned motor pump . Once the canned pump began to work , the heat generated by current losses of the stator windings ,core energy losses and eddy current losses in the shielding sleeve must be taken away by the circulating cooling liquid(Guan X.F,1995).

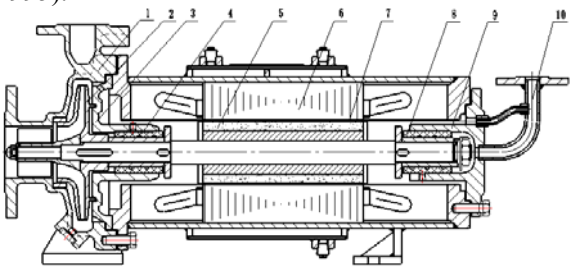

1 pump 2. Impeller 3. rear cover 4. left guide bearing 5. motor rotor 6. Stator 7. Shielding sleeve 8. right guide bearing 9. back cover plate 10. Circulating tube

Figure 1. Structure of permanent magnet canned pump

NUMERICAL SIMULATIONS

Flow Field

The model is a centrifugal pump, and its impeller has 6 vanes. The technical parameters of model pump are shown in Table 1.

The calculation domain is mainly composed of two parts, the static volute and the rotating impeller. In order to carry out a more accurate unsteady calculations , first of all steady simulation ought to be operated to supply initial conditions for the unsteady calculations(Ni et al,2006).

Table 1 Technical parameters of centrifugal pump

Flow rate	5m^3/h
Head	8m
Impeller inlet diameter	35mm
Impeller outside diameter	88mm
Outlet width of impeller	4mm
Volute inlet width	10mm

Based on these parameters , we modeled channel of impeller and volute case by 3D soft. In order to simulate flow field exactly, length of inlet and outlet taken 2-4 times of their diameter, model is shown as Figure 2. Un-structure tetrahedral grid with strong flexibility is adopted for the discretization of the geometry. The mesh in impeller has 58 4154 grids while that in casing has 126 1156 ones. Grids are shown as Figure 3.

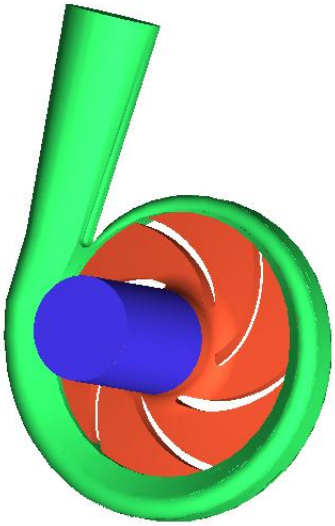

Figure 2. 3D models of impeller and volute

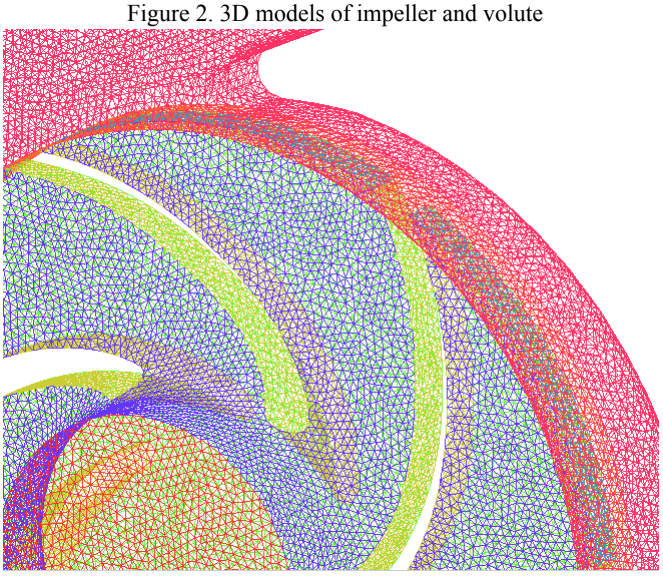

Figure 3. Grids of impeller and volute

3D Steady Flow

In FLUENT, RNG k -e turbulent flow model is chosen. The N-S equation with finite volume method is solved and SIMPLE arithmetic is adopted, which fits for steady flow. The boundary condition at pump inlet is velocity-inlet and its magnitude is computed from design point flow rate. The boundary condition at pump outlet is outflow. The solid walls such as blade surface, hub, shroud and casing surface should satisfy the non-slip condition and are assumed to be adiabatic. All the solid walls of impeller are rotating and the rotating speed is the same as impeller. The operation pressure is 101325 Pa. The numerical calculations are carried out with a multiple frame of reference approach, whereby the impeller flow field is solved in a rotating frame and the casing in a fixed one(Wang, et al,2003).

The simulated results of model pump are shown in Figure 4. The absolute velocity distribution of the midsection

in the internal flow field is shown in Figure 4(a) for the design flow rate. With the increasing of impeller radius, the absolute velocity in the impeller channel of the model pump increases. A vortex is shown by uneven distribution of the absolute velocity in the circumferential direction. With the appearance of vortex, it has proved the existence of pressure fluctuation. Figure 4(b) shows the distribution of static pressure. The static pressure of impeller end is lower than the one of places nearby blade suction side and blade pressure side. At the same radius, the pressure value of blade pressure side is greater than the value of suction side. In order to research the mechanism, it is necessary to analysis pressure fluctuation of these places.

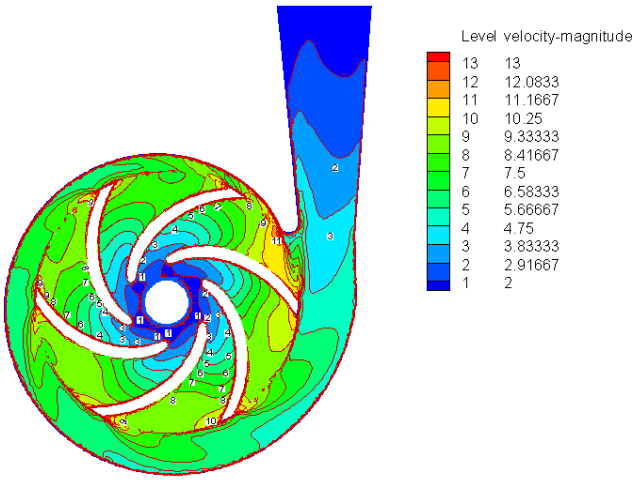

(a) The distribution of absolute velocity

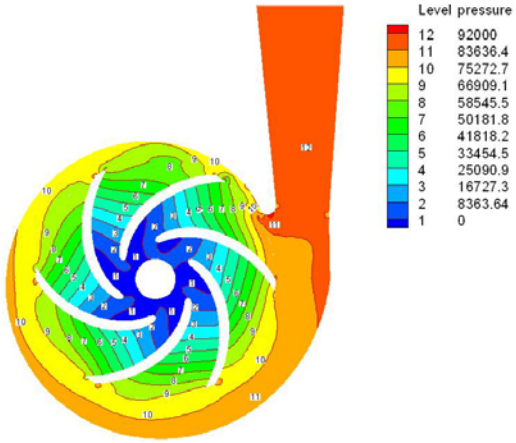

(b) The distribution of pressure

Figure 4. 3D steady flow simulated results of model pump

3D Unsteady Flow

In this calculation, the calculating period is the time duration for the impeller to rotate 360°. Setting one time step is corresponding to 3 degree of the impeller rotation. It means if the contents of one cycle of the impeller need to be understood, 120 times of such iteration calculation ought to be done (Yuan, et al,2009).

Blade passing frequency f is related to rotation speed n and blade number Z.

$$f = \frac{nZ}{60}$$

Pressure coefficient C_p:

$$C_p = \Delta p / \left(0.5 \rho U_2^2\right)$$

There, Δp is the difference value between the average static pressure and static pressure.

After impeller running for 10 cycles , pressure data begin to be collected. Figure 5 shows pressure fluctuations of the impeller exit on different operation conditions within the 11th rotation period. It shows the periodic distribution of pressure fluctuation. They are close to sinusoidal waveform. With the flowrate increase, periodic conditions are more obvious.

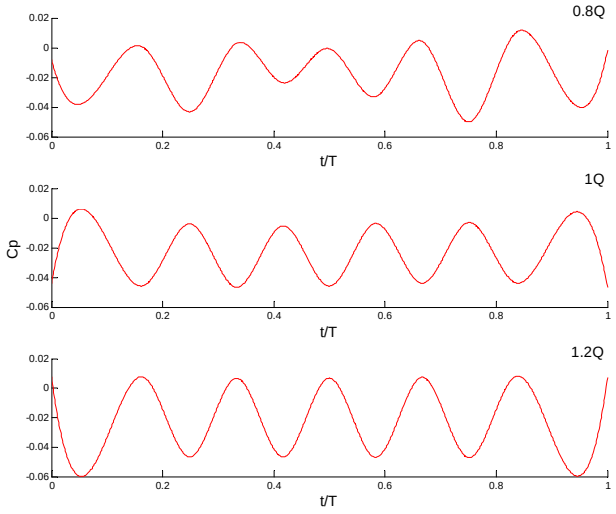

Figure 5. Pressure fluctuations at the impeller exit on different operation conditions

After FFT, the results of frequency spectra of pressure fluctuation obtained as shown in Figure 6. With the flowrate increasing, pressure fluctuation is more obvious under the blade passing frequency.

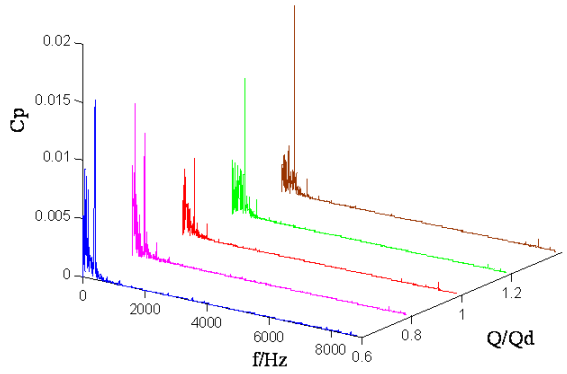

Figure 6. Frequency spectra of pressure fluctuation at the impeller exit on different operation conditions

There are also 4 indicator points in the blade pressure side and suction side as shown in Figure 7.

During 3D unsteady flow numerical simulation , PISO arithmetic replace SIMPLE.A sliding interface technique is applied to simulate the rotor-stator interaction.

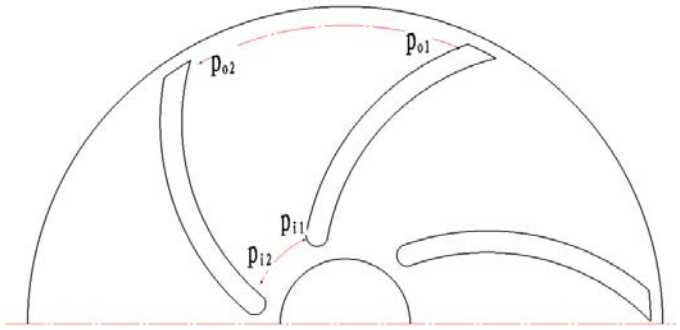

Figure 7. Indicator points in impeller flow passage

FFT processing is applied to the display of the pressure feature in frequency domain (XU C H, et al,2004). Figure 8 are the pressure fluctuation curves in frequency domain at both design and off-design points along with the indicator points . These results indicate that the pressure fluctuation around blades is very complex :

• Comparing Figure 8(a) and Figure 8(c),or Figure 8(b) and Figure 8(d) ,it shows that the value of the pulse amplitude on blade suction side is greater than the one on blade pressure .

• With the flow increases , the pulse amplitude are also increasing. For example in Figure 8(a), the value at $1.4Q_d$ is 4.78 times as high the value at design point.

• From the figure we can see that high-frequency pressure fluctuation occurs at the trailing edge of blade flow channel, the pressure fluctuation frequency of the point is 391.9Hz, sub-frequency is 783.8Hz, those frequencies are close to the blade passing frequency .

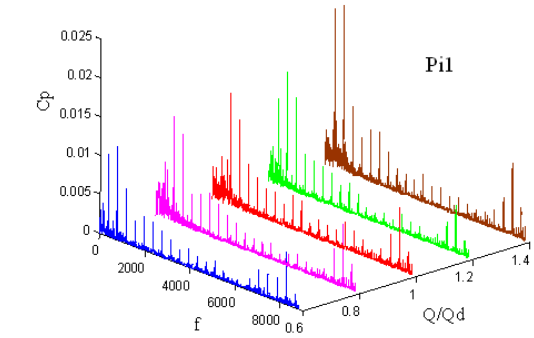

(a)

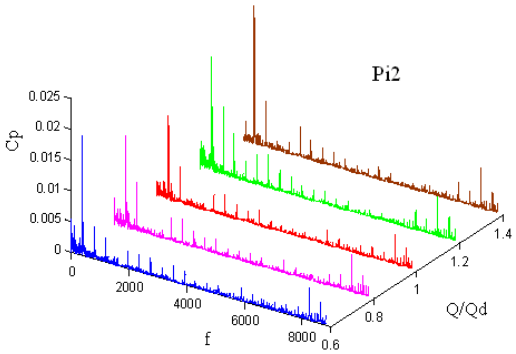

(b)

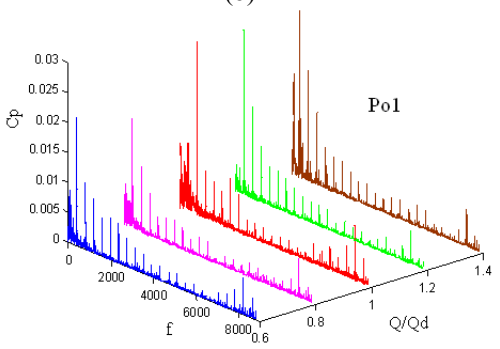

(c)

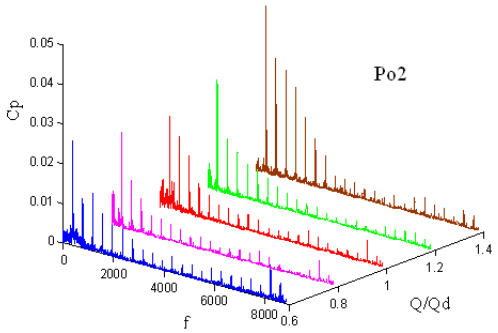

(d)

Figure 8 Frequency domain chart of pressure with different indicator points

Their fluctuating features are almost coincident with each other, which are similar to that tested by Nicholas et al (2003). All of the frequency spectrums show that the dominant frequencies simulated are approximate to the blade passing frequency.

Electromagnetic Field

After the completion of the design of hydraulic components, it is necessary to predict motor performance for improving the motor efficiency. The canned motor designed are applied by the design method of permanent magnet synchronous motor. The internal electromagnetic field of the motor is simulated with the ANSOFT software. The primary electromagnetic parameters of permanent magnet canned motor are shown in Table 2.

Table 2 Primary electromagnetic parameters of permanent magnet canned motor

Motor rated power	0.5kW
Motor rotational speed	3000rpm
Stator outer diameter	65 mm
Stator inner diameter	44 mm
Rotor outer diameter	40 mm
Rotor inner diameter	15mm
The lengths of core	60 mm
Slot number ratio	36/28

According to the electromagnetic parameters in Table 2, plotted the 2D modeling of canned motor in the ANSOFT. During the geometric modeling, considering the symmetry of the motor structure, the simulation only need to draw one polar distance size of the model. Geometric model of permanent magnet canned motor is shown in Figure 9.

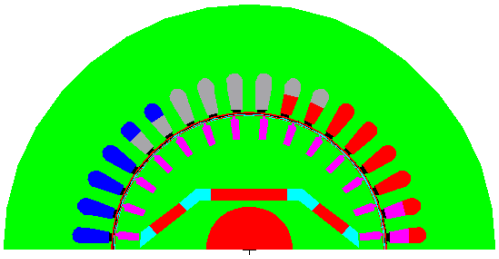

Figure 9 Geometric model of permanent magnet canned motor

The definition of material properties: stator and rotor core is used in Cold-rolled silicon steel DW315-50; magnet for N42SH; shielding sleeve for non-magnetic shielding metal materials, such as HASTELLOY-C; shaft for stainless steel material.

Set the boundary conditions and excitation source: when no-load, just set the motor main border, stator outer diameter auxiliary boundary value of zero boundary conditions; once load, in addition to setting the three-phase stator coil winding conditions and the end ring parameters.

Figure 10 shows magnetic line distribution of two different magnetic circuit structures in the anent magnetic canned motor . In Figure 10(a),at the sides of the rotor tooth and stator tooth there are not magnetic field lines passed. A large part of the rotor magnetic field lines form a loop in the rotor core. Therefore, magnetic flux leak very seriously in the U-type permanent magnet end, finally adversely affect the performance of the magnet motor; Figure 10(b), the distribution of magnetic lines in the magnetic shielding motor is more evenly. Most of the magnetic field lines reach the stator through the rotor, forming a stator - rotor magnetic field lines loop. Inverted U-type magnetic structure maximizes the using of permanent magnets. The least permanent magnet can be used to achieve the required performance of permanent magnet canned motor, thus the final prototype using this structure can save production costs.

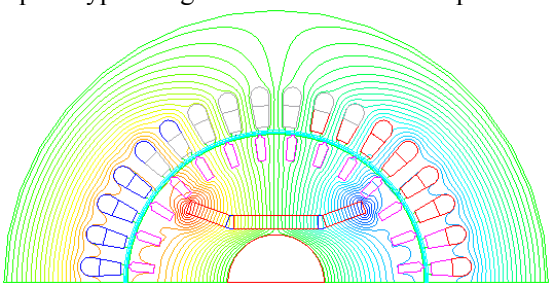

(a) U-type

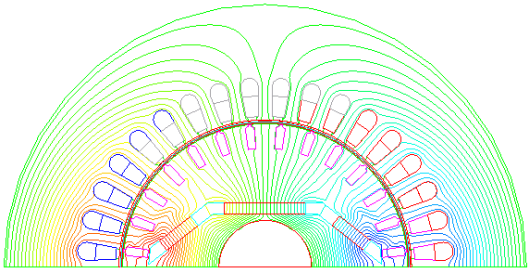

(b) Inverted U-type

Figure 10. Distribution of magnetic line in permanent magnet canned motor pump

In the ANSOFT-Post , the value of air-gap magnetic flux can be calculated. Figure 11 shows graph of air-gap magnetic flux in the motor. When the air gap δ = 2.0mm, the air-gap magnetic flux density Br is at the average of about 0.35T. This value is very close to the theoretical value. All of these show that the simulations are appropriate.

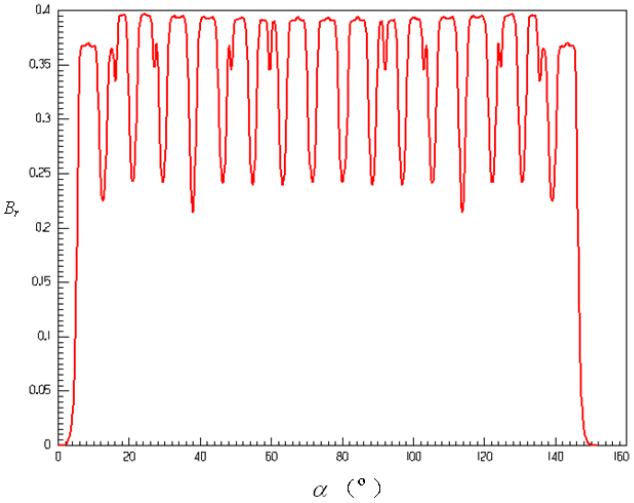

Figure 11. Graph of air-gap magnetic flux (δ=2.0mm)

EXPERIMENT

The pump was tested on a open test-bed, Figure 12 shows the instruments of the experiment. The measurements of flow, head, efficiency, performance are according to ISO 5198:1987.

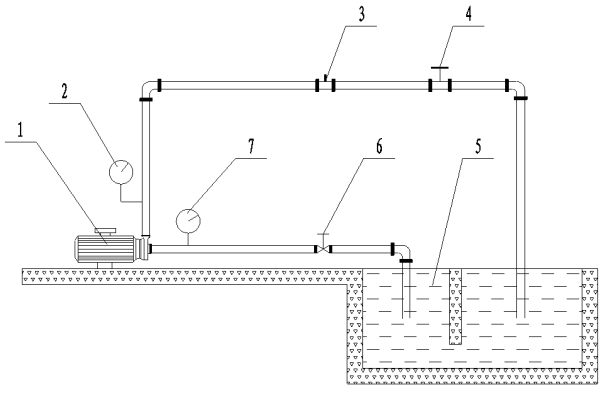

1-Canned pump 2- Outlet pressure gauge 3- Turbine flow meter
4- Outlet control valve 5-Pool 6- Inlet control Valve
7- Inlet pressure gauge

Figure 12. Schematic diagram of experimental setup

The experimental data and the value of numerical simulation are shown in Figure 13. Numerical simulation obtains the similar curve as the experimental test. At the design point, the simulation value of the head is close to experimental value.

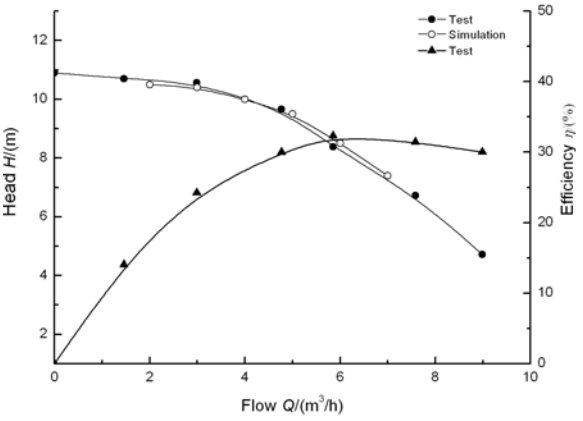

Figure 13. Performance curve of test pump

CONCLUSION

By the internal electromagnetic field simulation of permanent magnet canned motors, it can build an initial understanding of the permanent magnet rotor structure . Compared to U-type magnetic circuit structure, the inverted U-type is more conducive to reducing the magnetic flux leakage in the iron core tooth. In order to enhance the performance of the canned motor and shorten the design period, it is very necessary to do the further research on the permanent magnet rotor.

From 3D steady flow numerical simulation, the absolute velocity distribution is uneven in the circumferential distribution inside the impeller. At the impeller outlet, a lower static pressure zone appears in the middle of the impeller channel exit, while higher static pressure zones appear near the suction side and pressure side of the blade. Then the pressure fluctuation analysis of both blade suction side and pressure side by 3D unsteady flow numerical simulation explain pressure distribution. Finally, the simulation value of the head is closer to experimental data. Fluid numerical simulation can meet the requirements.

ACKNOWLEDGMENTS

The authors gratefully acknowledge the financial support of the National Science and Technology Pillar Program (No.2008BAF34B10).

REFERENCES

[1] Kong Fanyu, Chen Shiliang, Yuan Shouqi.Expermental Reaearch on Design of Circulating Loop of Canned Motor Pump[C].*The 7th Asian International conference on Fluid Machinery.Japan*:2003:2–8

[2] Kong Xianghua, Kong Fanyu, JI Jiangang. Calculation and experiment on canned motor pump[J]. *Drainage and Irrigation Machinery,* 2006,8(4):10～13

[3] Chen Hongxun, Guo Jiahong.Numerical simulation of 3-D turbulent flow in the multi-intakes sump of the pump station[J]. *Journal of Hydrodynamics,* 2007, 19(1): 42-47.

[4] Nicholas P, Poul S L, and Christian B J, 2003, Flow in a Centrifugal Pump Impeller at Design and Off-Design Conditions—Part I: Particle Image Velocimetry (PIV) and Laser Doppler Velocimetry (LDV) Measurements, *ASME Journal of Fluids Engineering,* 125(1): 61-72.

[5] Guan, X.F.,1995, Handbook of Modern Pumps, Space Navigation Press, Beijing.

[6] Ni Yongyan, Pan Zhongyong, and Li Hong, et al, 2006, Application of Characters of Discharge Pressure Fluctuation to Monitor of Centrifugal Pump, *Drainage and Irrigation Machinery,* 24(5): 40-43. (In Chinese)

[7] Wang H, Tsukamoto H, 2003, Experimental and Numerical Study of Unsteady Flow in a Diffuser Pump at Off-Design Conditions, *ASME Journal of Fluids Engineering,* 125(5): 767-778.

[8] Yuan Shouqi, Ni Yongyan, and Pan Zhongyong, et al,2009, Unsteady Turbulent Simulation and Pressure Fluctuation Analysis for Centrifugal Pumps, *Chinese Journal ofMechanical Engineering,* 22(1): 64-69.

[9] XU C H, Wu Y L, Chen N X et al, 2004, "Unsteady Blade-Row Interaction Calculation In High Speed Pump",*Chinese Journal of Mechanical Engineering,* Vol. 40(3) ,pp. 1-4 (In Chinese)